Microtubule transport

DOI: 10.1002/smll.200600410

Directing Transport of $CoFe_2O_4$-Functionalized Microtubules with Magnetic Fields**

Benjamin M. Hutchins, Mark Platt, William O. Hancock, and Mary Elizabeth Williams**

Control of the transport and organization of nano- and microscale materials and molecules is a continuing challenge in nanoscience and bio-microelectromechanical systems (MEMS) research. In eukaryotic cells these tasks are faithfully carried out by kinesin motor proteins and their associated microtubule tracks, which makes this motor an attractive candidate for actuation and transport in hybrid biological devices. However, control of the direction of microtubules transported by immobilized kinesin motors is a key hurdle to the implementation of this system. Magnetic fields are ideal for mechanically perturbing biological systems because they are easily controlled and noninvasive, but labeling proteins with magnetic particles can disrupt their biological function. Here we show that by selectively functionalizing microtubule segments with 20-nm $CoFe_2O_4$ magnetic nanoparticles, external magnetic fields can be used to control the transport direction of gliding microtubules without affecting their transport speed. These findings demonstrate a novel approach for manipulating kinesin-driven microtubule movements in vitro that can be extended to other protein systems.

In cells, kinesin motor proteins convert chemical energy derived from the hydrolysis of adenosine triphosphate (ATP) into mechanical energy to move intracellular cargo along microtubules, cylindrical polymers (25 nm in diameter) of the protein tubulin that act as intracellular conduits.[1] Conventional kinesin contains two motor domains that sequentially bind and hydrolyze ATP, thereby causing conformational changes that result in the protein and its cargo moving processively toward the fast-growing (plus) end of the microtubule.[2,3] This cellular transport system can be reconstituted with purified kinesin motors and microtubules in vitro and used either to move functionalized motors along immobilized microtubules or inverted to transport microtubules along motor-functionalized surfaces (Figure 1).[1] Chemical modifications of the kinesin and microtubule proteins enable selective labeling for the attachment of cargo, including quantum dots,[4–7] silica[8,9] and polymer[6] beads, and other inorganic nanoparticles.[10,11] These labeling schemes provide new opportunities to use biomolecular motors for the directed assembly of complex nanostructures as well as possible applications in protein tracking and force measurements.[8,9,12] Furthermore, the manipulation and observation of purified kinesins and microtubules in vitro allows investigations into the fundamental principles underlying cytoskeletal organization in cells.

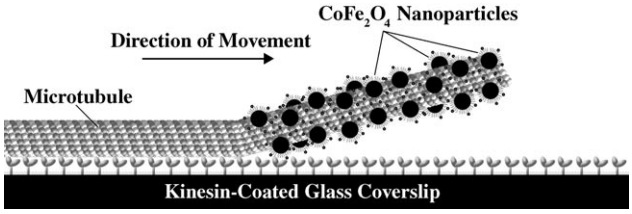

Figure 1. Schematic representation of a segmented microtubule, which is selectively biotinylated and labeled with magnetic $CoFe_2O_4$ nanoparticles on its leading end (minus end), being transported over a kinesin-modified glass surface.

A number of approaches have been used to control the direction of microtubules moving over kinesin-functionalized surfaces, including constraining microtubules in narrow or enclosed microfabricated channels[13–16] and reorienting microtubules by fluid flow[17] or electric fields.[18–20] These approaches all work on the principle that as a microtubule is transported over a surface of motors, the free front end is constantly searching for new motors to bind, so that bending the front segment to bind motors on one side will redirect the entire filament. While these existing tools are somewhat effective, they can be cumbersome and expensive to fabricate (for example, microchannels), or they nonselectively exert forces on all components of the system and are not ideal in microscale geometries (for example, fluid flow and dc electric fields). A recent report by van den Heuvel et al.[20] showed that dc electric fields can be used to steer kinesin-driven microtubules in microscale channels, but the electrodes must be placed millimeters from the sorting channels to avoid unwanted electrolysis. New techniques that complement and extend the current technologies should allow specific mechanical perturbations of selected components of the microtubule system and be adaptable to a range of experimental conditions and geometries.

Magnetic fields are especially well suited to perform these tasks without need for lithographic electrode or chan-

[*] B. M. Hutchins, Dr. M. Platt, Prof. M. E. Williams
Department of Chemistry
104 Chemistry Bldg.
The Pennsylvania State University
University Park, PA 16802 (USA)
Fax: (+1) 814-865-3292
E-mail: mbw@chem.psu.edu
Prof. W. O. Hancock
Department of Bioengineering
229 Hallowell Bldg.
The Pennsylvania State University
University Park, PA 16802 (USA)
Fax: (+1) 814-863-0490
E-mail: wohbio@engr.psu.edu

[**] This work was supported by The Pennsylvania State University Center for Nanoscale Science, a National Science Foundation Materials Research Science and Engineering Center (DMR0213623), and by a CAREER award from the National Science Foundation (to M.E.W., CHE0239-702).

Supporting information for this article (nanoparticle transmission electron micrographs and directed motility video footage) is available on the WWW under http://www.small-journal.com or from the author.

nel fabrication, or they may also be used together with microfabricated structures to perform bio-MEMS tasks. Magnetic nanoparticles are being explored as tools for cell and biomolecule separations, drug delivery, and magnetic imaging.[21] While micrometer-sized magnetic beads have been used to perturb cells[22] and to manipulate single rotary motor proteins by magnetic tweezers,[23,24] there has been little work with magnetic *nano*particles. In systems where protein–protein interactions are critical, the large size of microparticles (0.5 μm and larger) can be problematic,[6] thereby making nanoparticles attractive candidates for force generation, provided sufficient forces can be generated.

By functionalizing microtubules with magnetic nanoparticles, we show that external magnetic fields can be used to control the direction of microtubules moving along kinesin-functionalized surfaces. We recently demonstrated that microtubules labeled with $CoFe_2O_4$ nanoparticles will reorient in solution along the field lines of an external magnet and that this uniform alignment is preserved when they land on a kinesin-covered surface (Figure 2).[11] However, after the introduction of ATP to initiate transport, the microtubules move in random directions, and over time this movement erases the alignment pattern. Furthermore, the bulkiness of the attached nanoparticles and neutravidin inhibits the interaction of the kinesin motors with the microtubules and results in slower gliding speeds and reduced motility.[11,25] Thus, when weak magnetic-field strengths that are practical for use on a microscope stage (without noticeable magnetization of optics and stage components) are employed, the degree of magnetic-nanoparticle labeling that preserves microtubule function is insufficient to control the transport direction of the microtubules on the kinesin-covered surfaces.

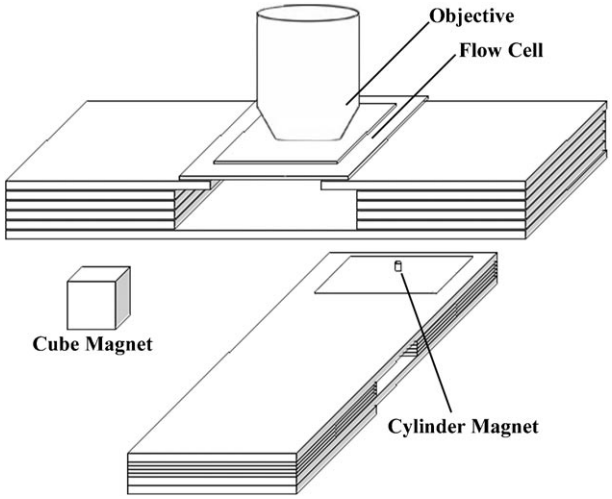

Figure 2. The experimental arrangement for magnetic surface preconcentration and directed motility experiments. A 60× water immersion objective was used to focus on the bottom of the flow cell (larger coverslip). Magnetic microtubules were preconcentrated with a 5-mm cube magnet and directed with a smaller 1-mm-diameter cylindrical magnet on a movable insert.

To enable magnetic control of the transport direction and to alleviate the decreased gliding speed of heavily particle-laden microtubules, we turned to the use of segmented microtubules that contain one unlabeled segment that binds optimally to motors and one segment maximally loaded with $CoFe_2O_4$ nanoparticles, which prevent any kinesin binding (Figure 1). In this way, the region of the microtubule that is influenced by the magnetic field can be localized to the front segment to maximize directional control. An image of magnetically labeled segmented microtubules in the absence of a magnetic field is shown in Figure 3A. Two visible domains are apparent: a bright rhodamine–tubulin segment and a dim biotin–tubulin segment. The decrease in fluorescence caused by the relatively lower density of rhodamine tags in the 80% biotinylated segment enables rapid verification of the segmented morphology.

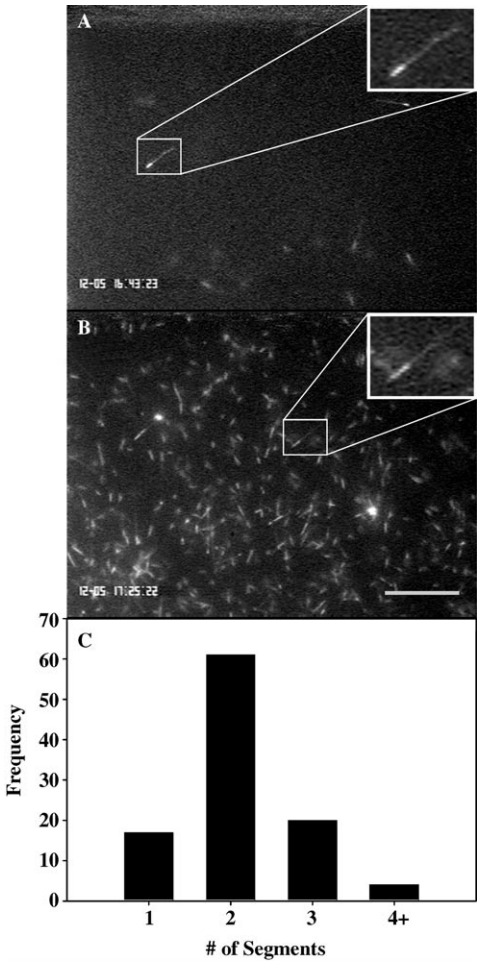

Figure 3. Fluorescence images of segmented microtubules (80% biotin-labeled leading end; unlabeled trailing end) bound to a kinesin-coated glass coverslip in A) the presence and B) the absence of an applied magnetic field. The scale bar represents 20 μm. The insets are 2.5× magnifications of the boxed areas. C) Plot of a typical population distribution of segmentation seen for microtubules magnetically preconcentrated on the surface.

The fluorescence image in Figure 3B shows the enhanced surface coverage when these $CoFe_2O_4$-labeled segmented microtubules are added to the kinesin-covered slide in the presence of a NdFeB cube magnet placed under the

flow cell. The distinction between the biotinylated (dim) and nonbiotinylated (bright) segments is again readily apparent. Consistent with our earlier report,[11] the applied magnetic field attracts the magnetically labeled microtubules and causes many more to bind to the surface. The large population of microtubules visible on the motor-covered surface allows a statistical assessment of the morphologies of the population of segmented microtubules. Although the method of inhibiting minus-end growth with *N*-ethylmaleimide-labeled tubulin (NEM-tubulin) is well established,[26,27] careful analysis of the microtubules on the surface (such as in the representative image shown in Figure 3B) indicates that the population is somewhat heterogeneous (Figure 3C). Microtubule breakage or failure to polymerize a second segment results in a fraction with one dim (biotinylated) segment, while nucleation of new microtubule seeds yields a fraction with one bright (nonbiotinylated) segment. A fraction of microtubules had three segments, a result indicating that the NEM-tubulin is unable to completely block the minus-end growth from every biotin-labeled microtubule seed. Freshly prepared NEM-tubulin minimizes, but does not eliminate, this effect. Finally, a small fraction of microtubules contained four segments, which presumably resulted from microtubule annealing, which has been observed previously.[28] For our experiments, this heterogeneity provides a convenient internal standard because unlabeled microtubules are unaffected by the presence of a magnetic field and microtubules with three segments show different behavior in applied magnetic fields (discussed below). Strict control over NEM-tubulin-regulated growth conditions (including the NEM-tubulin concentration, growth time, and seed concentration) may reduce the heterogeneity for applications in which only the two-segment morphology is desirable, and this is the subject of ongoing work in our laboratory.

To assess their functionality, the microtubules were pulled down to the surface in the presence of a magnetic field, the magnet was removed, and ATP was added to initiate movement. These microtubules moved at $(0.68 \pm 0.20)\ \mu m\,s^{-1}$ (mean ± standard deviation (SD), number of measurements (N) = 39), which compares favorably with the value of $(0.77 \pm 0.04)\ \mu m\,s^{-1}$ (N = 53) seen for control (unsegmented) microtubules. When the magnetic-field gradient was reapplied, the segmented microtubules moved with an average gliding speed of $(0.77 \pm 0.09)\ \mu m\,s^{-1}$ (N = 20). We attribute this small increase to population differences caused by the horizontal magnetic-field component preferentially detaching microtubules with shorter unlabeled segments, rather than to a forced acceleration (see force estimates below). In previous work with unsegmented microtubules, we found that when as little as 10% biotinylated tubulin was used, particle labeling reduced speeds by roughly half and labeling with higher biotin percentages completely inhibited movement.[25] Based on the near-native gliding speeds of these segmented microtubules, their movement is ascribed exclusively to the interaction of the unlabeled microtubule segments with the kinesin motors; the use of 80% biotinylated tubulin to maximize particle labeling completely blocks the interaction of those motors with the labeled segments. These findings are consistent with those with nanocrystalline quantum-dot-labeled microtubules, where mobility was optimal in a segmented construct.[4]

We next tested whether external magnetic fields could be used to control the transport *direction* of these magnetically functionalized microtubules. As conventional kinesin is a plus-end-directed motor[29] and the particle labeling is on the minus-end segment, the magnetic segment is expected to be the *leading* portion of the moving microtubule. The bright segments (nonbiotinylated tubulin) can easily be discerned from the dim, nanoparticle-labeled segments (Figure 3A). In the presence of ATP, it was confirmed that every microtubule containing one nanoparticle-labeled segment and one unlabeled segment moved with the nanoparticle-labeled (dimmer) segment leading. We further noted that the biotinylated portion frequently moved out of the focal plane of the microscope, which is indicative of unbinding from the kinesin-modified surface, while the trailing (unlabeled) end of the microtubule maintained contact with the kinesin surface and thus continued microtubule transport. Since the leading segment is magnetically functionalized and does not interact with surface-bound kinesin motors, this is the ideal geometry for using an external magnetic field to redirect the microtubule leading ends and thereby control the direction of the kinesin-driven microtubules.

The images shown in Figure 4 are representative frames from a video (available in the Supporting Information) acquired when a small cylindrical magnet was placed directly below the flow cell (one coverslip thickness, ≈175 μm from the motor surface) during the motility assay (Figure 2). Unbound magnetic nanoparticles in solution can interact with the magnetic field and induce fluid flow that could potentially alter the trajectory of surface-bound microtubules by exerting a viscous drag force. Therefore, to eliminate any possible flow, excess magnetic material was flushed out of the flow cell chamber with 1 μM ATP buffer solution. (This lower concentration of ATP is needed to retain bound microtubules and prevent them from washing out of the cell.) Short nonbiotinylated (that is, not magnetically labeled) microtubules were subsequently added as fluorescent tracers (easily distinguished by focusing into the solution) in a solution containing 1 mM ATP. The surface-bound segmented microtubules immediately began to move, and the position of the magnet was varied to change the magnitude and direction of the magnetic field in the flow cell.

As the position of the magnet was varied (indicated by the arrows in Figure 4), the magnetic particles bound to the leading segment exert a force orthogonal to the direction of travel, thereby bending the leading segment and the first portion of the trailing (unlabeled) segment. This results in the leading end of the unlabeled segment binding motors on one side, and as the microtubule moves (over micrometer distances) this bias results in a net change in the transport direction. In all cases, the magnetic-field-induced bending of the magnetic segment was nearly instantaneous, but a few micrometers of travel (taking a few seconds) were required to turn the entire filament and regain a straight trajectory.

Despite the changes in transport *direction*, the microtubule gliding *speed* was not affected by changes in the loca-

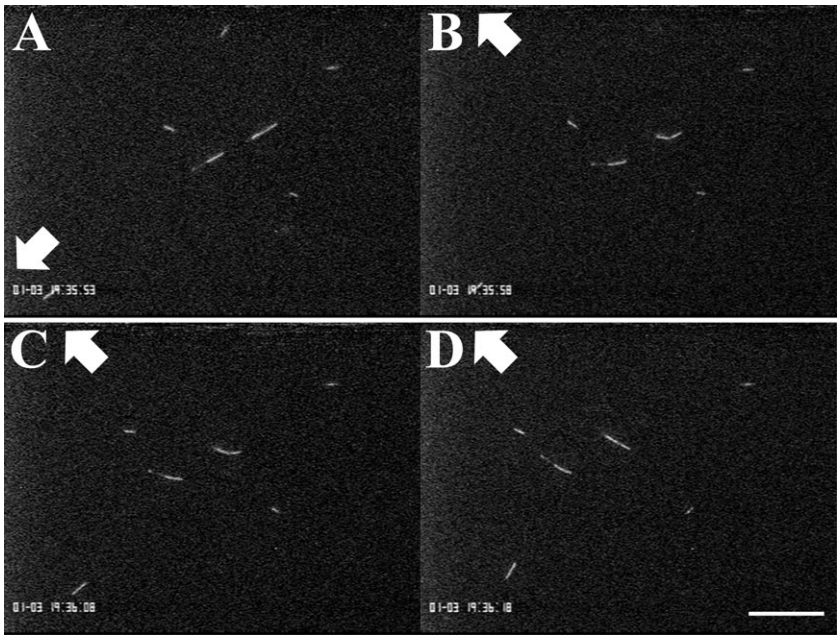

Figure 4. Four screen-captured images from a fluorescence microscopy video acquired during a microtubule gliding assay with the magnetically labeled segmented microtubules. The position of the magnet is changed during the experiment: the arrows indicate the direction to the center of the magnet for each frame. The scale bar represents 20 μm. The time lapses between frames are as follows: A→B = 5 s, B→C and C→D = 10 s.

tion of the magnet. For instance, a single guided microtubule maintained a speed of $(0.69 \pm 0.11)\ \mu m\,s^{-1}$ (mean ± SD) when magnetically redirected seven times. Furthermore, the speed was independent of the distance between the magnet and microtubule, a fact that is supported by our previous results showing that magnetic forces are insufficient to overcome the motor forces (see the force discussion below).[25] Directed transport was observed for several microtubules per screen, but only for microtubules containing one magnetically labeled segment and one nonlabeled segment. Microtubules consisting entirely of particle-functionalized tubulin did not bind to the surface, and microtubules with no magnetic nanoparticles attached were unaffected by changes in the location of the magnet. Importantly, the particle-free fluorescent tracer microtubules in solution did not move in response to magnetic-field changes, a result indicating that there was no net solution flow. Changes in the external magnetic field did not affect multisegmented microtubules that resulted from polymerization of particle-free tubulin on both ends of the biotinylated seeds. This observation implies that the magnetic-field forces on the particle-labeled segment are much smaller than the kinesin forces holding the front segment of these microtubules to the surface.

Based on the known mechanical properties of microtubules and the kinesin–microtubule bond, we can estimate the magnitude of the forces involved in this microtubule redirection. A change in the location of the magnet caused the front segment of the microtubules to bend, which can be modeled as a flexible cantilever (the free microtubule segment) attached to a rigid base (the motor-bound trailing segment). The uniformly distributed force (F) required to bend a beam of length L by a distance y_{max} at its end is described by Equation (1),[30] where the flexural rigidity (EI) of taxol-stabilized microtubules has been measured to be $2 \times 10^{-23}\ N\,m^2$.[31]

$$F = \frac{8EIy_{max}}{L^3} \quad (1)$$

From microtubule redirection measurements such as those shown in Figure 4, we observed 5-μm segments of microtubules that bent in the order of 3 μm at the tip. This corresponds to a force of 4 pN over the entire 5-μm segment, which is likely to be an underestimate because Equation (1) applies to only small deflections. In rare cases, radii of curvature as small as 1 μm were observed. An upper limit of the force can be estimated from the observation that microtubules with a particle-free segment on their front end were not redirected by the applied magnetic fields: these ≈1 μm segments interact with approximately 1–10 motors and kinesin-unbinding forces have been measured in the 5–15 pN range,[32,33] so an upper limit on the force that would be required to bend these is roughly 100 pN. The magnetic-field forces on these microtubule segments are therefore in the range of single-motor stall forces for conventional kinesin.[12,34] Based on an estimate that 1000 20-nm particles are packed on a 5-μm segment of a microtubule with a diameter of 25 nm,[35] then a 10 pN force scales to 10 fN per magnetic nanoparticle. Since microtubules with very long magnetic segments (>12 μm) were not observed, forces above this upper limit were not attained.

These experiments conclusively demonstrate that external magnetic fields can be used to control the direction of magnetically labeled microtubules driven by kinesin motors in vitro. These hybrid nanobiological systems are capable of rapid transport at near wild-type speeds and have implications in nanometer-scale manipulations through biologically derived forces and magnetic-induced guidance. The ≈10 fN forces produced by single nanoparticles are most likely insufficient to affect protein function, but multiple labels acting in concert can exert substantial forces and serve as handles for external control of protein function. These results could impact on the use of biomotors for separation, manipulation, and assembly of nanoscale components, potentially over distances approaching millimeters. Owing to the inherent parallel nature of microtubule-based separations and force generation, this approach provides an enticing alternative to serial methods such as optical tweezers.

Magnetically labeled microtubules additionally provide a new tool for in vitro investigations of the role of microtubules and motors in important cellular processes such as cell division, axonal transport, and flagellar motility.

Experimental Section

Instrumentation: Fluorescence microscopy was performed on an upright Nikon E600 microscope (1.2 NA, 60× water immersion objective) coupled to a Genwac GW-902H CCD camera. The video was recorded with a Panasonic AG-MD835 video cassette recorder onto VHS videotapes for offline analysis. Transmission electron micrographs (see the Supporting Information) were obtained on a JEOL JEM 1200 EXII instrument operating at 80 kV with an attached high-resolution Tietz F224 digital camera. Two shapes of NdFeB permanent magnets (Engineered Concepts, Inc., Birmingham, AL) were employed: a 5-mm cube with a field strength of 0.45 T, and a 1-mm diameter, 2-mm tall cylinder with a field strength of 0.4 T. Field gradients were measured with a hand-held gaussmeter (Magnetic Instrumentation, Inc.; Model 907).

Chemicals and reagents: All chemicals were purchased from standard commercial sources and used without further purification.

Synthesis of CoFe2O4 nanoparticles: Biotin-functionalized CoFe2O4 nanoparticles were prepared and encapsulated in a 5% biotin-tagged micelle as previously described.[] The nanoparticles were used at a concentration of 3 mg mL^{-1} in freshly prepared BRB12 buffer (12 mm 1,4-piperazinediethanesulfonic acid (PIPES), 1 mm MgCl2, 1 mm ethylene glycol-bis(2-aminoethylether)-N,N,N′,N′-tetraacetic acid (EGTA), pH 6.8).

Kinesin and microtubule preparation: HexaHis-tagged Drosophila melanogaster conventional full-length kinesin was expressed in Escherichia coli, purified according to published methods,[3] and used at a concentration of 5 μg mL^{-1}. Tubulin was purified from freshly harvested bovine brain tissue and labeled with rhodamine or biotin by using standard techniques.[] Preparation of biotin-functionalized microtubules was performed by copolymerization of biotinylated tubulin and rhodamine-containing tubulin (25% rhodamine-labeled/unlabeled tubulin) at 37 °C in BRB80 buffer (80 mm PIPES, 1 mm MgCl2, 1 mm EGTA, pH 6.8) with 1 mm guanosine triphosphate (GTP), 4 mm MgCl2, and 5% (v/v) dimethylsulfoxide (DMSO) for 20 min. The microtubules were diluted 100-fold (320 nm tubulin dimer) with BRB80 buffer containing 10 μm paclitaxel. Segmented microtubules were prepared similarly to previously reported methods,[] by shearing biotinylated microtubules[11] through a 30 gauge needle in paclitaxel-free BRB80 buffer and adding them to a solution of 3.2 μm rhodamine-labeled tubulin (1:3 rhodamine-labeled/unlabeled tubulin) and 6 μm NEM-tubulin[26,38] in BRB80 with 4 mm MgCl2, 1 mm GTP, and 5% DMSO. This solution was incubated for 20 min at 37 °C, such that polymerization occurred from the microtubule plus end but was blocked by NEM-tubulin at the minus end.[] The resulting segmented microtubules were stabilized by diluting them 100-fold in a solution of BRB80 containing 10 μm paclitaxel.

Magnetic labeling: Segmented microtubules were labeled with CoFe2O4 nanoparticles by incubating microtubules (320 nm tubulin dimer; 10 μL) with neutravidin (8.3 μm; 10 μL) for 5 min and then adding stock nanoparticle solution (3 mg mL^{-1}; 5 μL). For kinesin motility experiments, this solution (10 μL) was added to freshly prepared motility solution (90 μL of BRB80 containing 0.2 mg mL^{-1} casein, 10 μm paclitaxel, 20 mm glucose, 20 μg mL^{-1} glucose oxidase, 8 μg mL^{-1} catalase, and 0.5% β-mercaptoethanol (bME)) with 1 μm or 1 mm ATP, as noted in the text.

Microtubule gliding assays: Standard microtubule gliding assays were performed by using fluorescence microscopy to visualize the kinesin-driven transport of rhodamine-labeled microtubules in the presence of 1 mm ATP. All motility experiments were performed in flow cells constructed from two pieces of double-sided tape sandwiched between two coverslips, as shown in Figure 2. Prior to each experiment, a new flow cell was constructed, and the interior surfaces were perfused with 0.5 mg mL^{-1} casein for 5 min and then exposed to 5 μg mL^{-1} kinesin[3] in buffer (BRB80, 0.2 mg mL^{-1} casein, 1 mm ATP) for 5 min.

Magnetically directed motility studies: Directed motility studies were performed by using a modified flow-cell holder with a glass insert, shown in Figure 2. A 1-mm-diameter cylinder magnet mounted on the tip of the glass insert provided a magnetic field that was movable by sliding the insert along the underside of the flow cell. Magnetic preconcentration was performed in this same cell (although not under the microscope), by placing a 5-mm (edge-length) cube magnet under the flow cell, adding magnetic microtubules, and waiting for 5 min before removing the magnet. The flow cell was then flushed with the first buffer (5 volumes, 100 μL; BRB80, 0.2 mg mL^{-1} casein, 10 μm paclitaxel, 1 μm ATP), followed by the second buffer (20 μL; 99.5 μL BRB80 containing 0.2 mg mL^{-1} casein, 10 μm paclitaxel, 20 mm glucose, 20 μg mL^{-1} glucose oxidase, 8 μg mL^{-1} catalase, 0.5% bME, with 0.5 μL short/sheared microtubules added as flow tracers).

We observed the structure and behavior of two-segment microtubules bound to the kinesin surface that were successfully redirected and noted a small dependence on the length of each segment. The length of the free magnetic ends ranged from 2–11 μm with a mean of (5 ± 3) μm (mean ± SD, N = 13). The absence of very long leading ends (> 12 μm) may be due to the rinsing procedure (described above) that was used to remove unbound particles: the fluid flow produces viscous forces that preferentially act on longer nonbound microtubule segments, thereby causing detachment of the remaining bound segment. For the same reason, microtubules with short segments of nonlabeled tubulin may not be sufficiently attached to the motor surface to remain bound through the rinse procedure, as manifested in a minimum 4.5 μm length of the unlabeled segments and an average length of (6 ± 2) μm (mean ± SD, N = 13).

Keywords:
kinesin · magnetic fields · microtubules · nanoparticles · transport

[1] R. D. Vale, T. S. Reese, M. P. Sheetz, *Cell* **1985**, *42*, 39.
[2] J. Howard, *Annu. Rev. Physiol.* **1996**, *58*, 703.

[3] W. O. Hancock, J. Howard, *J. Cell Biol.* **1998**, *140*, 1395.
[4] G. D. Bachand, S. B. Rivera, A. K. Boal, J. Gaudioso, J. Liu, B. C. Bunker, *Nano Lett.* **2004**, *4*, 817.
[5] X. Nan, P. A. Sims, P. Chen, X. S. Xie, *J. Phys. Chem. B* **2005**, *109*, 24220.
[6] M. Bachand, A. M. Trent, B. C. Bunker, G. D. Bachand, *J. Nanosci. Nanotechnol.* **2005**, *5*, 718.
[7] G. Muthukrishnan, B. M. Hutchins, M. E. Williams, W. O. Hancock, *Small* **2006**, *2*, 626.
[8] S. M. Block, L. S. B. Goldstein, B. J. Schnapp, *Nature* **1990**, *348*, 348.
[9] D. L. Coy, M. Wagenbach, J. Howard, *J. Biol. Chem.* **1999**, *274*, 3667.
[10] S. Behrens, K. Rahn, W. Habicht, K.-J. Böhm, H. Rosner, E. Dinjus, E. Unger, *Adv. Mater.* **2002**, *14*, 1621.
[11] M. Platt, G. Muthukrishnan, W. O. Hancock, M. E. Williams, *J. Am. Chem. Soc.* **2005**, *127*, 15686.
[12] K. Svoboda, C. F. Schmidt, B. J. Schnapp, S. M. Block, *Nature* **1993**, *365*, 721.
[13] Y. Hiratsuka, T. Tada, K. Oiwa, T. Kanayama, T. Q. P. Uyeda, *Biophys. J.* **2001**, *81*, 1555.
[14] S. G. Moorjani, L. Jia, T. N. Jackson, W. O. Hancock, *Nano Lett.* **2003**, *3*, 633.
[15] H. Hess, C. M. Matzke, R. K. Doot, J. Clemmens, G. D. Bachand, B. C. Bunker, V. Vogel, *Nano Lett.* **2003**, *3*, 1651.
[16] Y.-M. Huang, M. Uppalapati, W. O. Hancock, T. N. Jackson, *IEEE Trans. Adv. Packag.* **2005**, *28*, 564.
[17] R. Stracke, K. J. Böhm, J. Burgold, H.-J. Schacht, E. Unger, *Nanotechnology* **2000**, *11*, 52.
[18] K. Boehm, N. Mavromatos, A. Michette, R. Stracke, E. Unger, *Electromagn. Biol. Med.* **2005**, *24*, 319.
[19] M. G. L. van den Heuvel, C. T. Butcher, S. G. Lemay, S. Diez, C. Dekker, *Nano Lett.* **2005**, *5*, 235.
[20] M. G. L. van den Heuvel, M. P. de Graaff, C. Dekker, *Science* **2006**, *312*, 910.
[21] Q. A. Pankhurst, J. Connolly, S. K. Jones, J. Dobson, *J. Phys. D* **2003**, *36*, R167.
[22] N. Wang, J. P. Butler, D. E. Ingber, *Science* **1993**, *260*, 1124.
[23] Y. Rondelez, G. Tresset, T. Nakashima, Y. Kato-Yamada, H. Fujita, S. Takeuchi, H. Noji, *Nature* **2005**, *433*, 773.
[24] Y. Hirono-Hara, K. Ishizuka, K. Kinosita, Jr., M. Yoshida, H. Noji, *Proc. Natl. Acad. Sci. USA* **2005**, *102*, 4288.
[25] B. M. Hutchins, M. Platt, W. O. Hancock, M. E. Williams, *Micro Nano Lett.* **2006**, *1*, 47.
[26] A. Hyman, D. Drechsel, D. Kellogg, S. Salser, K. Sawin, P. Steffen, L. Wordeman, T. Mitchison, *Methods Enzymol.* **1991**, *196*, 478.
[27] T. B. Brown, W. O. Hancock, *Nano Lett.* **2002**, *2*, 1131.
[28] S. W. Rothwell, W. A. Grasser, D. B. Murphy, *J. Cell Biol.* **1986**, *102*, 619.
[29] R. D. Vale, B. J. Schnapp, T. Mitchison, E. Steuer, T. S. Reese, M. P. Sheetz, *Cell* **1985**, *43*, 623.
[30] R. W. Fitzgerald, *Mechanics of Materials*, Addison-Wesley, Reading, MA, **1982**.
[31] F. Gittes, B. Mickey, J. Nettleton, J. Howard, *J. Cell Biol.* **1993**, *120*, 923.
[32] K. Kawaguchi, S. Ishiwata, *Science* **2001**, *291*, 667.
[33] N. J. Carter, R. A. Cross, *Nature* **2005**, *435*, 308.
[34] E. Meyhofer, J. Howard, *Proc. Natl. Acad. Sci. USA* **1995**, *92*, 574.
[35] A hexagonally close-packed surface contains 26% empty space, so a fully laden microtubule with length L will have a maximum number of particles that is equal to $0.74\{[2L(M+P)]/(P^2)\}$, where M and P are the radii of the microtubule and nanoparticle, respectively. Therefore, a 5-μm microtubule segment could have a maximum of 1665 particles, while 1000 nanoparticles represents as a conservative estimate.
[36] S. G. Grancharov, H. Zeng, S. Sun, S. X. Wang, S. O'Brien, C. B. Murray, J. R. Kirtley, G. A. Held, *J. Phys. Chem. B* **2005**, *109*, 13030.
[37] R. C. Williams, Jr., J. C. Lee, *Methods Enzymol.* **1982**, *85*, 376.
[38] NEM–tubulin is prepared as 60 μM purified, unlabeled tubulin in BRB80 buffer with 1 mM *N*-ethylmaleimide (NEM), 0.1 mM GTP, and 8 mM β-mercaptoethanol (bME).

Received: August 10, 2006
Published online on November 29, 2006

